

# Flow separation control by off surface elements

L.L.M. Veldhuis <sup>\*</sup> and M. van der Steen <sup>†\*</sup>

*Delft University of Technology, the Netherlands*

Comparative wind tunnel experiments were performed on passive flow separation control on a flat plate model equipped with a flap. The purpose of these tests was to investigate the flow control capabilities of off-surface mounted elements. A comparison was made of delta-shaped vortex generators of 1 to 1/3 boundary layer height and cylinders close to the wall. Surface pressure as well as PIV measurements were performed to investigate the influence of the layout of the VGs as well as the diameter of the cylinder and the position of the elements.

The results showed that the off-surface devices performed better than the on-surface VGs for the fully separated case, and were equally good in improving the state of boundary layer that is on the verge of separation. It was also found that the off-surface devices could be positioned over a wider range with respect to the separation point. The experiments furthermore indicated that for the optimum cylinder configuration the vortex shedding frequency was consistent with the frequencies found in literature on periodic flow excitation.

## Nomenclature

$c_p$	pressure coefficient, $c_p = (p - p_\infty)/q_\infty$
$d$	horizontal distance
$d^*$	dimensionless distance between control element and separation line, $d^* = d/\delta$
$D$	cylinder diameter
$D^*$	dimensionless cylinder diameter, $D^* = D/\delta$
$h$	vertical distance to wall
$h^*$	dimensionless vertical position of control element, $h^* = h/\delta$
$p$	static pressure
$q$	dynamic pressure
$V$	flow speed
$\delta$	Boundary layer thickness
$\phi$	flap angle
<i>Indices</i>	
$\infty$	undisturbed value

## I. Introduction

OVER the past decades several innovative techniques to control flow separation over airfoils have been proposed. In recent years especially the research on active flow control methods has received interest. The application of active blowing, suction and the utilization of zero mass transfer synthetic jets (SJA)<sup>1-3</sup> have shown to be capable of postponing the separation to some extent. However, the practical implementation of these active methods may lead to an unwanted increase in mass and degradation of the wing's structural integrity (SJA). Furthermore there will be an increased power demand to drive pumps or excite piezo-electrical systems and associated hardware. Although attractive from the point of further improvement opportunities, many active systems have not matured to be incorporated in modern transport aircraft currently developed.

<sup>\*</sup>Associate professor, Faculty of Aerospace Engineering, Kluyverweg 1, 2626 HS, the Netherlands, AIAA member

<sup>†</sup>MSc student, Faculty of Aerospace Engineering, Kluyverweg 1, 2626 HS, the Netherlands

In this respect it is attractive to revisit the possible passive control methods, like vortex generators, that are available to provide an efficient means of flow separation control. At Delft University a research program has started aimed at developing novel *passive* control techniques and compare them with modern techniques like surface actuator and plasma actuators. In this paper the initial experimental research on off-surface control elements,<sup>4</sup> performed in a low speed windtunnel, will be addressed. The goal of this part of the project is to get further insight in the possibilities to use the wing trailing edge as an actuator support structure. From the flap point of view this configuration provides a means of off-surface placement of control elements. This enables to position the elements in an optimized position in the high energy gap flow (Fig. 1).

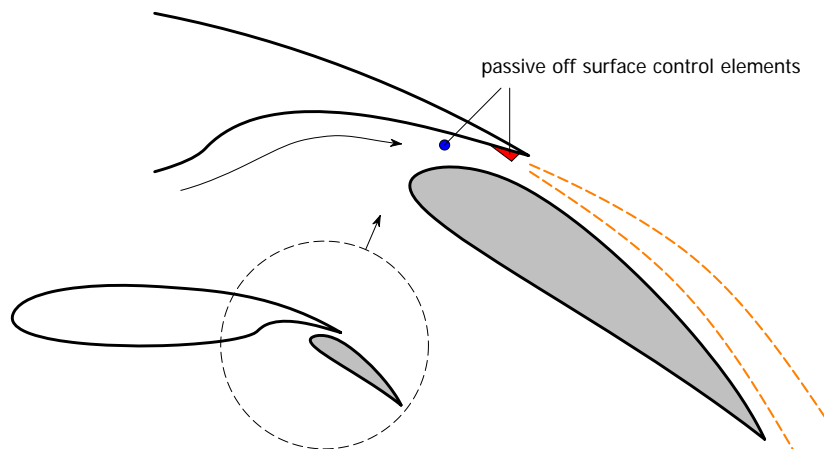


**Figure 1.** Application of off-surface elements to control flow separation over a flap.

## II. Off surface flow separation control

All flow separation control methods work by improving the state of the boundary layer to make it more resistant to a pressure gradient, and thus delay or even eliminate separation. Conventional vortex generators do this by mixing the flow inside the boundary layer with higher-momentum flow from outside the boundary layer, by means of longitudinal vortices.<sup>5,6</sup> The vortex generators are placed on the surface of the model, and the vortices that are created by the devices continuously swirl slowed-down air out of the boundary layer, and fresh outside air into it.

A similar approach is to introduce longitudinal vortices from the outside flow into the boundary layer. This technique could be useful when dealing, for instance, with diffuser flows, or a flow around a wing-flap configuration. One way of doing this is by simply placing vortex generators on top of or under the trailing edge of the main wing element to prevent flow separation on the flap.

In the current studies a simpler configuration is examined. In doing so, the vortex generators are entirely located in the free flow, while on-surface vortex generators are located within the boundary layer of the aerodynamic body on which they are located. Off-surface placement should therefore lead to higher vortex strength for the same device. Apart from mixing inside and outside boundary layer flow with longitudinal vortices one may also use lateral vortices to accomplish this.<sup>7-9</sup> These vortices have different decay characteristics, but can also be used for flow separation control. They also, by introducing a swirling motion, mix the air from inside the boundary layer with air from outside. The vortices can either be generated from the surface of the model, for instance by means of a mechanism with an oscillating plate, or from outside the boundary layer. One could use a similar oscillating plate, but these have the disadvantage that an external power supply is necessary. Cylinders, on the other hand, will shed a Von Kármán vortex street without

external power, i.e. passively. If a cylinder is positioned in such a way that its vortex street will interact with the boundary layer on the model, it can be used to add momentum to the boundary layer, and so prevent flow separation. This can be seen as the passive variation on periodic flow excitation. Apart from the unsteady flow effects that are generated by a cylinder the pressure field at the location may be influenced by suppressing the suction peak at the start of separation line leading to postponement of separation.

### III. Test setup

#### A. Model

The model that was investigated consists of a plate with an elliptical nose shape and a movable trailing edge flap (fig. 2). This simplified setup was chosen to maintain the separation at a fixed location which allows easy comparison of the various control techniques. Moreover the utilization of the flat plate model made the positioning of both on-surface and off-surface elements easier than would be the case for an airfoil shaped model. The flap of the model is equipped with 16 surface taps to acquire the pressure distribution. The flap could be deflected over  $\phi = 0^\circ$  to  $40^\circ$  to produce either attached, partly separated or fully separated flow. All experiments were performed in a turbulent boundary layer where the transition point was fixed

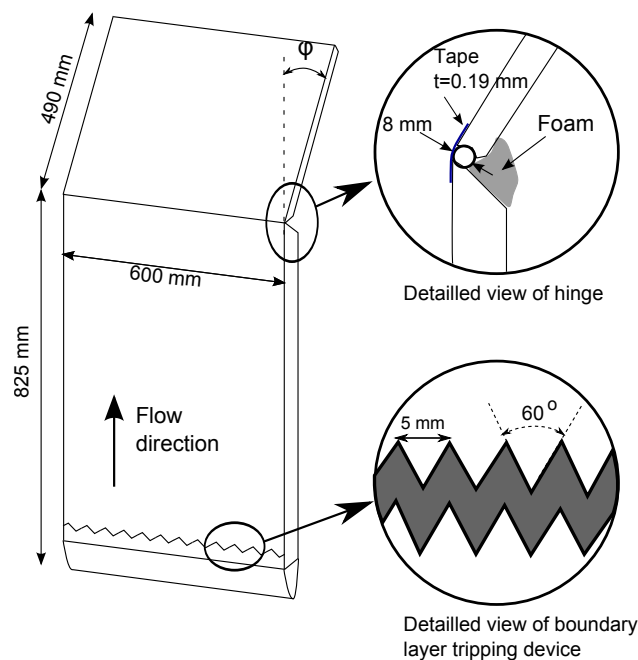


Figure 2. Windtunnel model dimensions and geometry.

close to the elliptical nose by applying Zig-Zag tape (thickness  $t = 1\text{ mm}$ , top angle  $\psi = 60^\circ$ ). The state of the boundary layer was determined using a stethoscope. In the tested velocity range (approximately 20 to 26  $m/s$ ) the flow showed transition in less than 10  $mm$  behind the tripping device over the entire width of the model.

#### B. Windtunnel and equipment

Experimental investigations were performed in a low speed windtunnel which blows air in vertical direction over the flapped plate (Fig. 3). To determine the behaviour of the boundary layer surface pressure measurements were performed over the flap. Besides this, flow surveys were performed using 2D PIV and Hot Wire measurements. Boundary layer velocity profiles were measured with a dedicated BL-probe. The wind speed was changed between 5  $m/s$  and 30  $m/s$ .

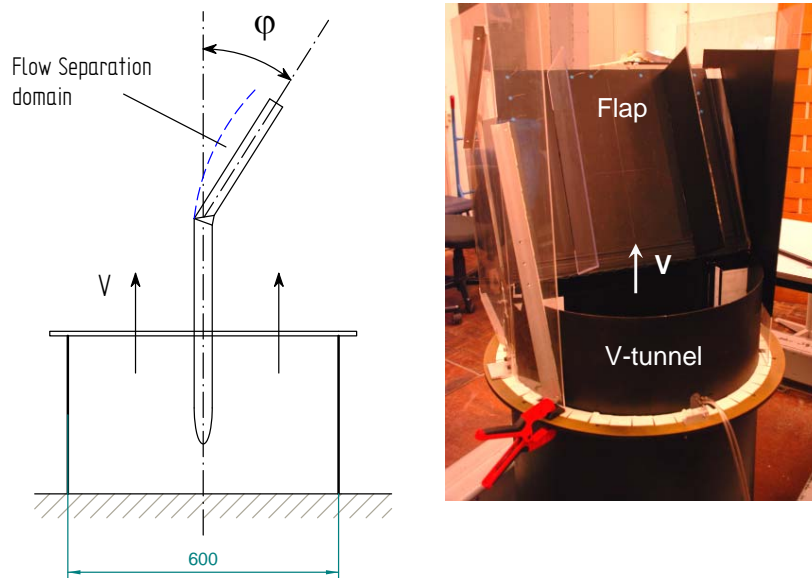


Figure 3. Windtunnel model; Layout and geometry (left); Photograph (right).

### C. PIV setup

PIV experiments have been performed for two flap angles. The laser sheet was produced by a Quantal Twins CFR-200 which composed of two pulsed ND:Yag lasers that produce aligned beams with a wavelength of  $1024\text{ nm}$  and a pulse duration of  $7\text{ ns}$ . Seeding was generated with a Safex Twin Fog Generator producing  $1\text{ }\mu\text{m}$  particles. The fields of view (FOV) in which the flow was analyzed are depicted in fig. 4. The corresponding experimental setups are shown in fig. 5. It must be noted that a similar setup was made for  $\phi = 28^\circ$  as the one depicted in but with different side plates.

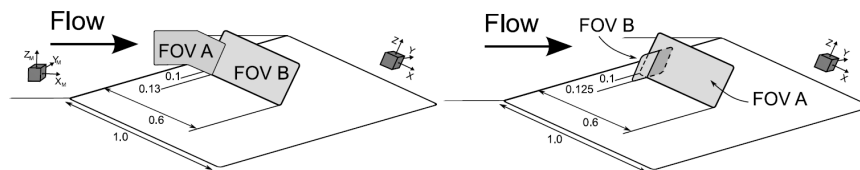


Figure 4. Fields of view setup of the PIV measurements.  $\phi = 28^\circ$  (left) and  $\phi = 32^\circ$  (right).

### D. Passive control elements

The effect of several flow control elements was compared with the turbulent baseline flow without control devices:

- On-surface vortex generators
- Off-surface vortex generators
- Cylinders

Standard VG's are known to be very effective in mixing the high energy outer flow into the boundary layer, hence leading to significant reduction of separation. In total three types of vortex generator configurations were used:

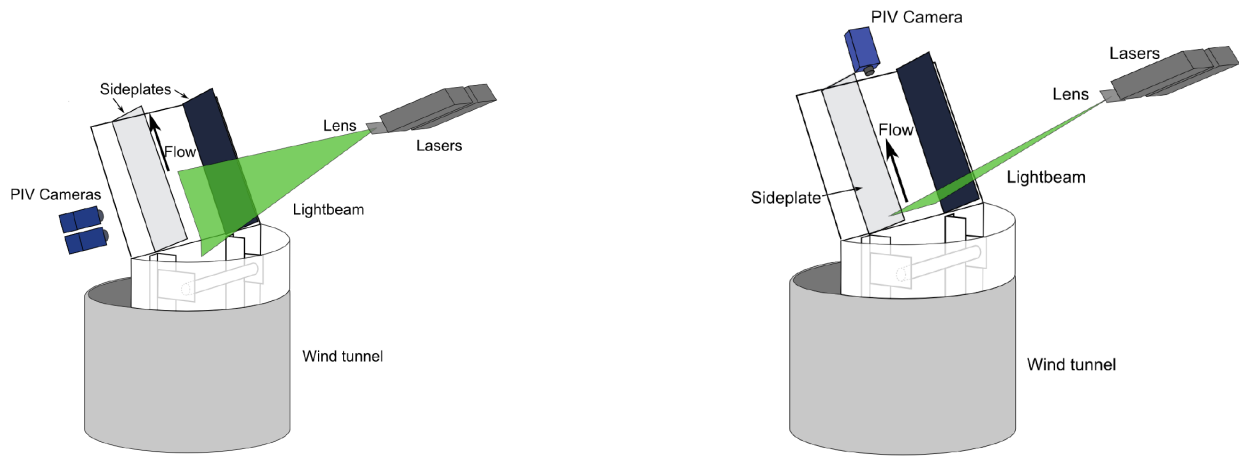


Figure 5. Schematic setup for PIV measurement in FOV A (left) and FOV B (right) for  $\phi = 32^\circ$ .

- $\delta$ -sized vortex generators that produce counter-rotating vortices
- $\delta$ -sized vortex generators that produce co-rotating vortices
- Counter-rotating Micro VGs (with a height of approximately  $\frac{1}{3}\delta$ )

The counter-rotating VGs and Micro VGs were tested in an on- and off-surface mode while the co-rotating VGs were only applied on-surface.

All tested VGs have the same basis shape, as depicted in side-view in fig. 6. The long side of the VG is set at  $\beta = 18^\circ$  with respect to the undisturbed flow direction.



Figure 6. Schematic layout of VG model used (left) and fabrication method from a rectangular metal sheet (right).

The VGs were fabricated by sharply bending a rectangular plate of thin material (a  $0.2\text{ mm}$  thick aluminium sheet) along a diagonal line, such that two perpendicular planes are formed. The VGs are simply attached to the surface by a double sided self-adhesive tape.

A counter-rotating VG configuration is described by several parameters (fig. 7):

- The spacing between two VGs in a pair,  $s$
- The distance between two vortex pairs,  $\lambda$
- The distance between the most downstream part of the vortex generator and the separation line,  $d$

Cylinders of different diameters were used with the purpose of utilizing the von Kármán vortex street to postpone separation. A sketch of the applied elements combined with their range of application is presented in Fig. 8.

## IV. Results

From an extensive matrix of flap angles and flow speeds two values were selected for further research:  $\phi = 28^\circ$  and  $\phi = 32^\circ$ . At  $\phi = 28^\circ$  the boundary layer over the flap is at the verge of separation (velocity

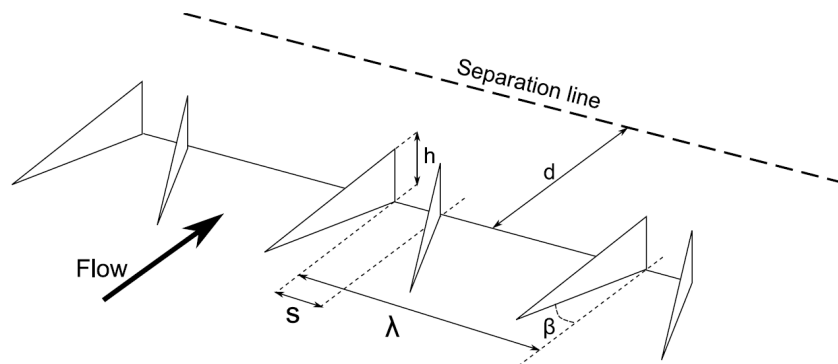


Figure 7. 3D view and representative parameters of the VGs.

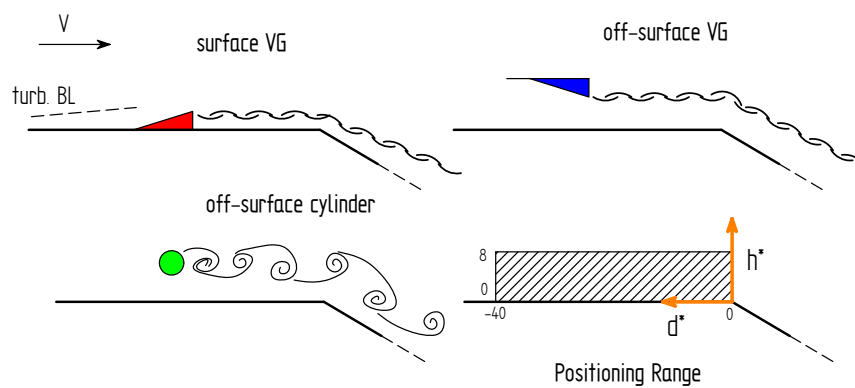


Figure 8. Flow control elements applied both on- and off-surface.

distribution inflection point near the wall) while  $\phi = 32^\circ$  shows a fully separated flow over the entire flap. All test were run at a flow speed of  $V = 24 \text{ m/s}$ .

### A. Reference case: VGs on-surface

**STANDARD VGs** The pressure distributions for the  $\phi = 28^\circ$  case shows that the boundary benefits of most of the passive elements that were applied, i.e. the differences of variations in spacing and streamwise position is very small as is evidenced by the pressure distributions presented in fig. 9 and 10. In these figures 'baseline' indicates the model without VGs installed. Only for a position very close to the separation point the pressure distribution showed minor improvement (not shown) which is due to the fact that the streamwise vortices do not have enough time to energize the lower part of the boundary layer.

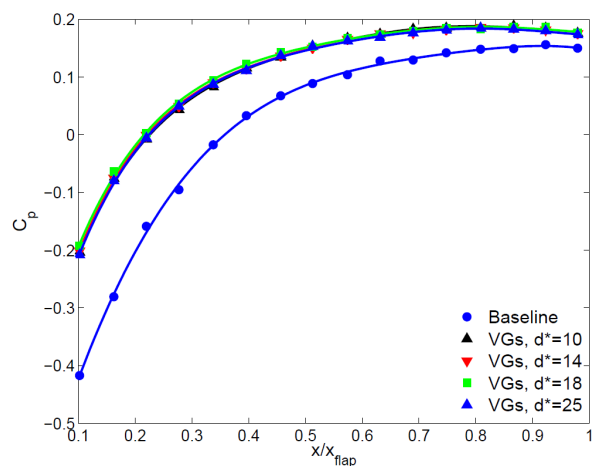


Figure 9. Effect of distance between counter rotating VGs and the separation point on the flap pressure distribution;  $(s, h) = (2h, 6h), \phi = 28^\circ$ .

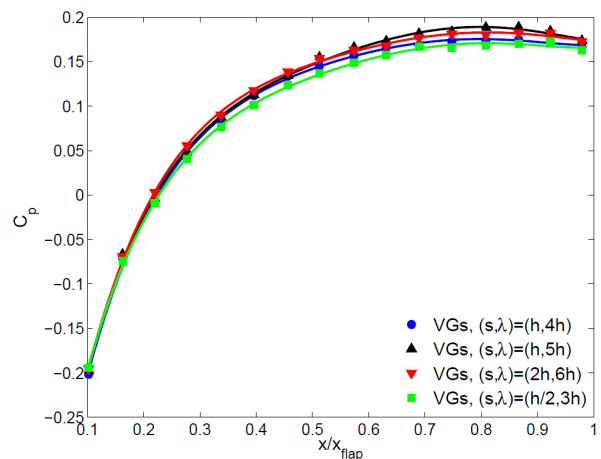


Figure 10. Effect of the spacing of counter-rotating VGs on the flap pressure distribution;  $\phi = 28^\circ$

For this reason all subsequent discussions on the results are limited to the  $\phi = 32^\circ$  case only. Some typical pressure distributions for the VG case are presented for  $\phi = 32^\circ$  in fig. 11. As can be seen, the baseline model exhibits fully separated flow (flat  $c_p$ ) over the flap while the VG's prevent separation completely for different values of the reduced distance  $d^* \leq 18$ . At  $d^* = 18$  the vortices produced by the VGs apparently have lost too much energy due to diffusion that flow separation can not be prevented over the entire flap.

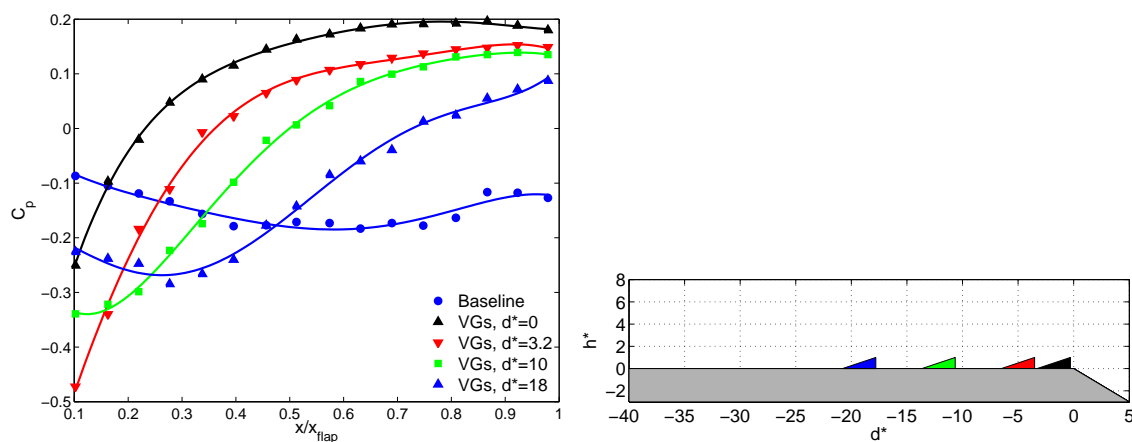
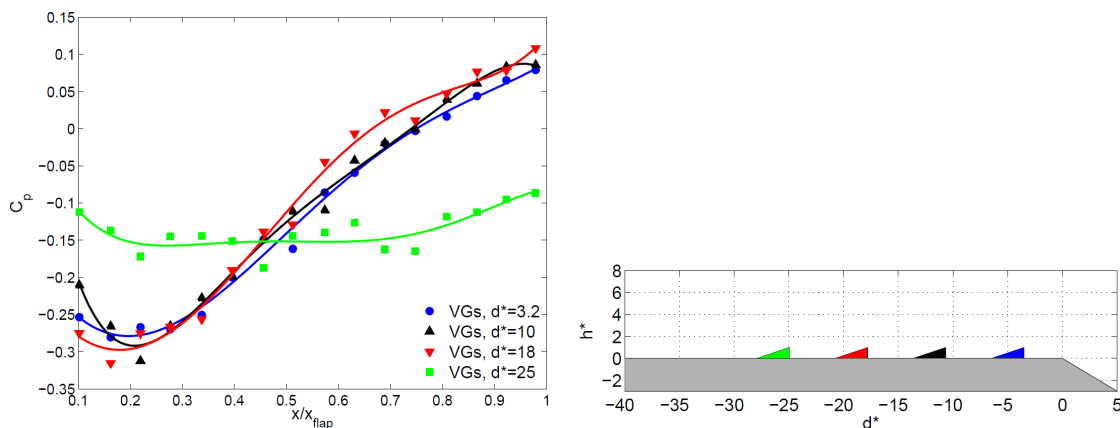


Figure 11. Effect of the distance between counter-rotating VG's and the separation point on the pressure distribution on the flap;  $(s, \lambda) = (h, \frac{9}{2}h); \phi = 32^\circ$ .

**CO-ROTATING VORTICES** Fig. 12 shows the pressure distribution with co-rotating VGs installed. It seems that VGs of this type are unsuitable for removing separation for a flow situation with given severe and abrupt adverse pressure gradient. This can be attributed to the fact that co-rotating VGs initially produce weaker vortices than counter-rotating VGs. However the co-rotating vortices remain closer to the wall which results in maintaining their strength over larger distances. Hence co-rotating VGs may be most useful in mild pressure gradients when the separation point is not exactly known in advance.



**Figure 12.** Effect of the distance between co-rotating VGs and the separation point on the pressure distribution on the flap. VGs spacing is  $\lambda = 3h$ ;  $\phi = 32^\circ$ .

**MICRO VGs** Fig. 13 shows the pressure distribution on the flap with Micro VGs installed. It is clear that the VGs must be placed as close to the separation point as possible, and increasing the distance immediately results in less favorable pressure distribution. However, the Micro VGs can successfully postpone or even eliminate separation, provided that the separation point is known in advance. If one compares the pressure distribution obtained by placing regular and Micro VGs directly in front of the separation point, it turns out that the standard VGs produce a much better pressure recovery for  $\frac{x}{L} > 0.35$ , but the Micro VGs seem slightly more effective on short distances  $d^*$ .

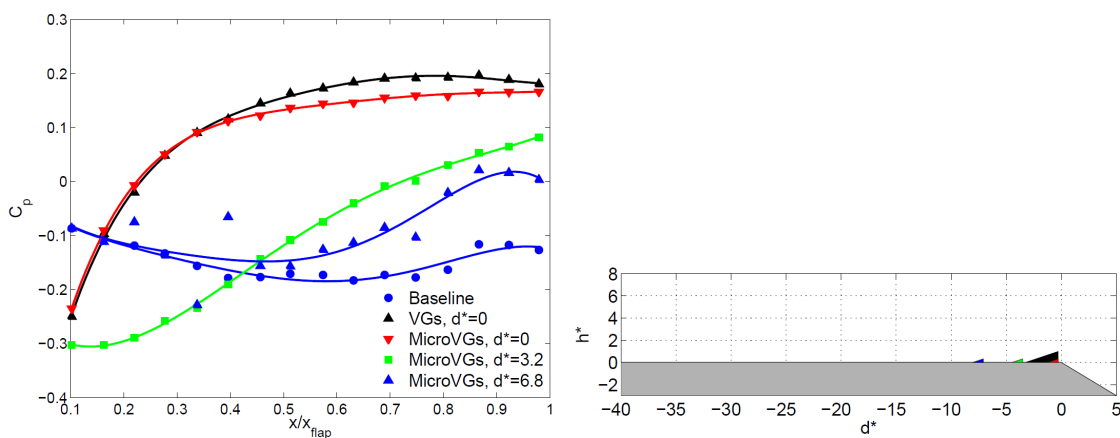


**Figure 13.** Effect of the distance between MicroVGs and the separation point on the pressure distribution on the flap;  $\phi = 32^\circ$ .

Table 1 lists the optimum vortex generator configurations found in this research. For comparison results from literature are given in table 2. As can be seen the parameters found for  $\phi = 28^\circ$  agree well with those found in literature. This means that even though there is no fully separated flow (the boundary layer is on the very verge of separation), this case is representative for flow separation control positions. The optimum parameters found for  $\phi = 32^\circ$  differ somewhat from the parameters found in literature: the devices are

positioned a little closer together, and the distance to the separation point is typically smaller. This can be explained by the fact that the separation for this case is not so much caused by a gradual adverse pressure gradient, but mainly by the geometry of the model (sharp corner at the start of the flap).

**Table 1. Optimum VG configurations found in this research.**

$\phi$	VG type	$\beta$	$h$	$\frac{\lambda}{h}$	$\frac{d}{\lambda}$
28°	counter-rotating VGs	18°	$\delta$	5-6	10-25
	co-rotating VGs	18°	$\delta$	3	18-32
	counter-rotating micro VGs	18°	$\delta/3$	4.5	0-10
32°	counter-rotating VGs	18°	$\delta$	4.5	0
	co-rotating VGs	not effective			
	counter-rotating micro VGs	18°	$\delta/3$	4.5	0

**Table 2. Optimum VG configurations from literature.**

Reference	VG type	$\beta$	$h$	$\frac{\lambda}{h}$	$\frac{d}{\lambda}$
Taylor (1950)	counter-rotating VGs	16°	$\delta$	5-12	10-30
Artois (2005)	counter-rotating VGs	16.7°	$\delta$	6.7	20-32
van der Jagt (2008)	counter-rotating VGs	17°	$\delta/3$	7	20
van der Jagt (2008)	counter-rotating micro VGs	17°	$\delta/2$	6.5	3
Lin et al (1990)	counter-rotating micro VGs	23°	$\delta/5 - \delta/5$	6.5	1-10

## B. Off surface elements

**STANDARD AND MICRO VGs** In fig. 14 the pressure distributions of different off-surface standard VGs are compared. The configurations of fig. 14a are peculiar because the tips of the vortex generators almost touch the model surface, which is not optimal for the formation of the vortices. Despite this the data show that the flow is kept attached by the vortices at the two closest positions. However, at  $d^* > 16$ , the flow is already fully separated.

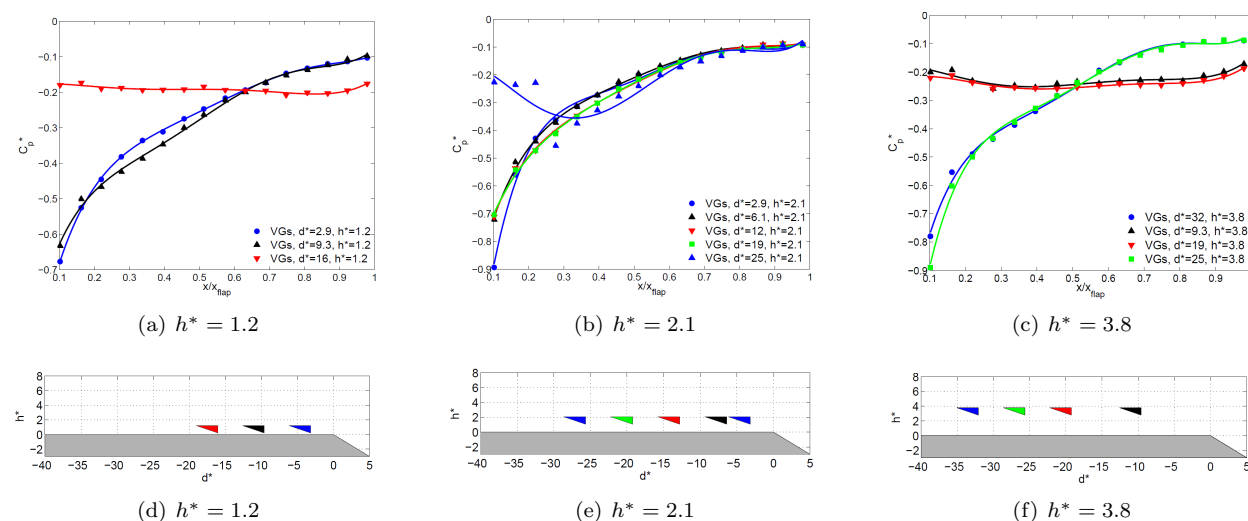


**Figure 14. Pressure distributions for off-surface VGs for different vertical positions.**

Increasing the height a little and allowing for a space of approximately  $\delta$  between the VG tips and the model produces pressure distributions as shown in fig. 14b. The flow is now kept attached for a wider range of horizontal positions, and the optimum point (out of the depicted plots) seems to lie at  $d^* = 6.1$ , which is

still quite close to the separation point. The last standard VG configuration was at  $h^* = 3.8$  (fig. 14c). Note that in this case the vortex generators closest to the separation point seem to be unable to maintain attached flow, while the VGs further away do. The one positioned furthest from the separation point now performs best. This can be explained by the fact that the vortices produced by the VGs with small  $d^*$  did not reach the boundary layer to interact with it, and are thus unable to postpone separation. This is schematically depicted in fig. 15.

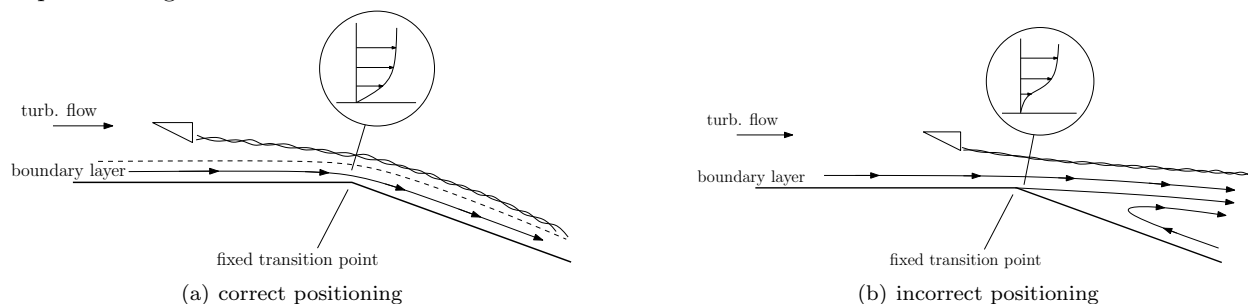


**Figure 15. Positioning of off-surface vortex generators with schematically depicted vortex path and boundary layer profile. The vortex of the aft positioned VG does not reach the separation point.**

For micro VGs the only configurations that maintained attached flow were at  $d^* = 1.2$ . There is a very obvious range for working positions. Moving too close to the separation point will again cause the vortices to pass over the low momentum part of the boundary layer, and will therefore not result in mixing of the surface boundary layer. Moving too far away leads to weakened the vortices which result in complete separation. The vortex generators at  $d^* = 7.7$  and  $d^* = 8.5$  perform equally well, and maintain fully attached flow.

**CYLINDERS** Four different cylinder diameters were tested. The smallest, with  $D^* = 0.43$  was unable to maintain attached flow, regardless of its position. In fig. 16 the pressure distribution of some of the tested cylinder configurations is presented.

The thin cylinder of  $D^* = 0.79$  (fig. 16a) was only capable of maintaining attached flow for  $h^* = 1.6$ . For both  $d^* = 9.3$  and 12 the pressure distribution is nearly identical, but moving the cylinder further away to  $d^* = 19$  results in a separated flow, probably because the vortices decay too much over that distance. It is interesting to notice that moving closer to the separation decreases the effectiveness of the cylinder at short range but produces a (slightly) better flow further downstream. The thicker cylinder of  $D^* = 0.79$  has a somewhat larger range of applicability (fig. 16b). Due to its larger diameter the shed vortices are stronger and attached flow is maintained up to  $d^* = 19$ . The larger cylinders  $D^* = 1.5$  and 2.2 show an even larger range, in terms of  $d^*$  and  $h^*$ , over which separation is postponed. The same observation can be made as for the cylinder with  $D^* = 0.8$  the closer position performs worse around the corner, but has a slightly better pressure recovery further downstream. It was found that for the  $D^* = 2.2$  cylinder at  $h^* = 3.1$ , moving the cylinder close to the separation point does not lead to separated flow. In this case the cylinder produces a wake which is large enough to already interact with the boundary layer before the separation point is reached. It is, however, unclear whether the effect that prevents flow separation is the unsteady effect of the vortex street interacting with the boundary layer, or the steady effect of pressure relieve at the corner.

In Fig. 17 the best vortex generator and cylinder configurations are compared. The two configurations that show the 'best' recovery are the cylinder with  $D^* = 2.2$  and off-surface,  $\delta$ -sized vortex generators. The optimum positions for each category have also been collected in Table 3. It becomes clear that a larger cylinder size allows (and sometimes forces) one to chose a higher position above the wall. These results indicate that off-surface flow separation control can lead to better results than on-surface control, and that a wider range of positions for the device will maintain attached flow. This makes off-surface flow separation control not only more effective, but also more flexible than on-surface flow separation control.

### C. PIV data

From a large number of PIV data for various setups of the model only a limited number is presented herein. Examples of typical PIV images that were obtained during this study are shown in Fig 18. The vectors fields depict velocity profiles which are composed of  $u$  and  $w$  (respectively parallel and perpendicular to the

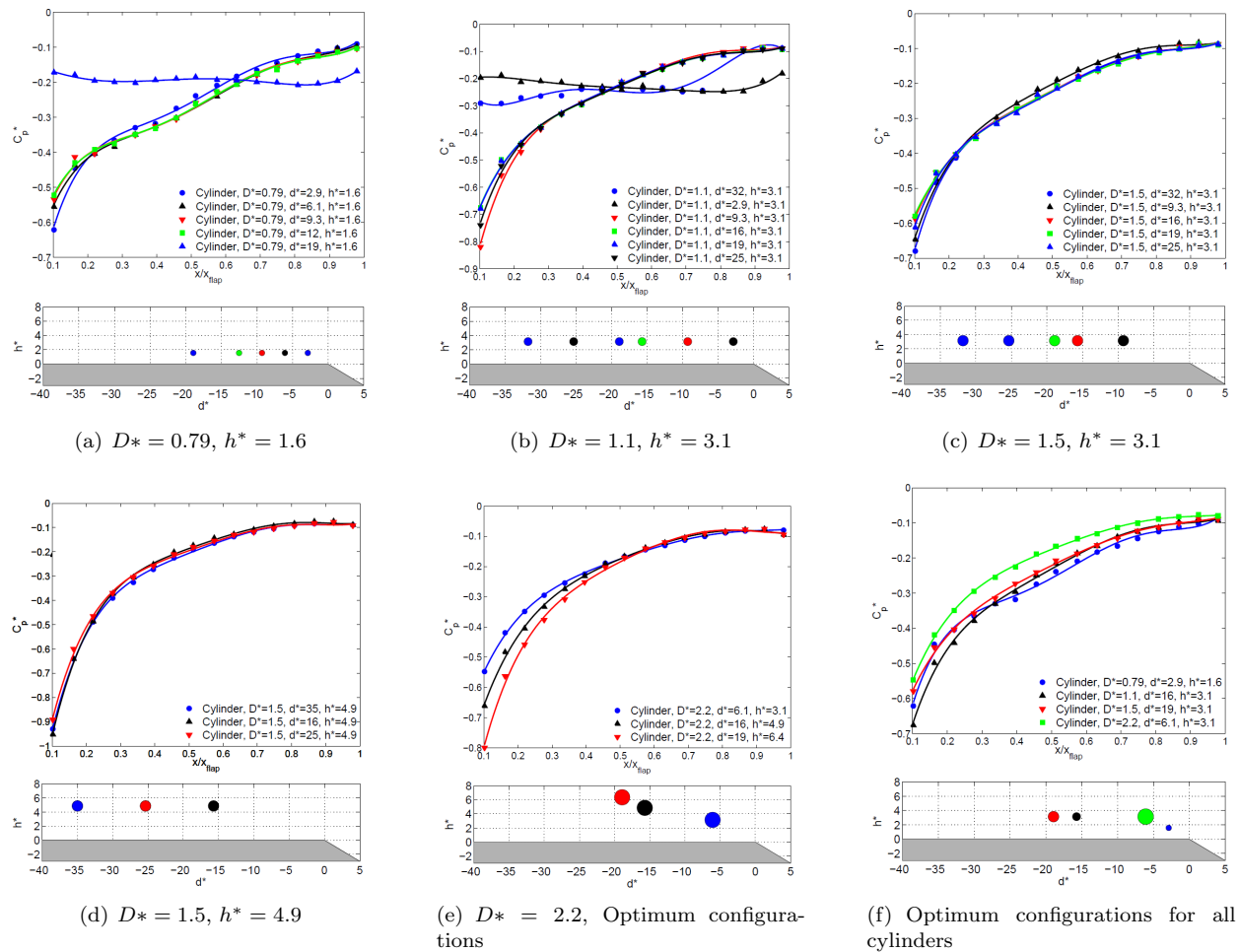


Figure 16. Flap pressure distributions for different off-surface cylinder configurations.

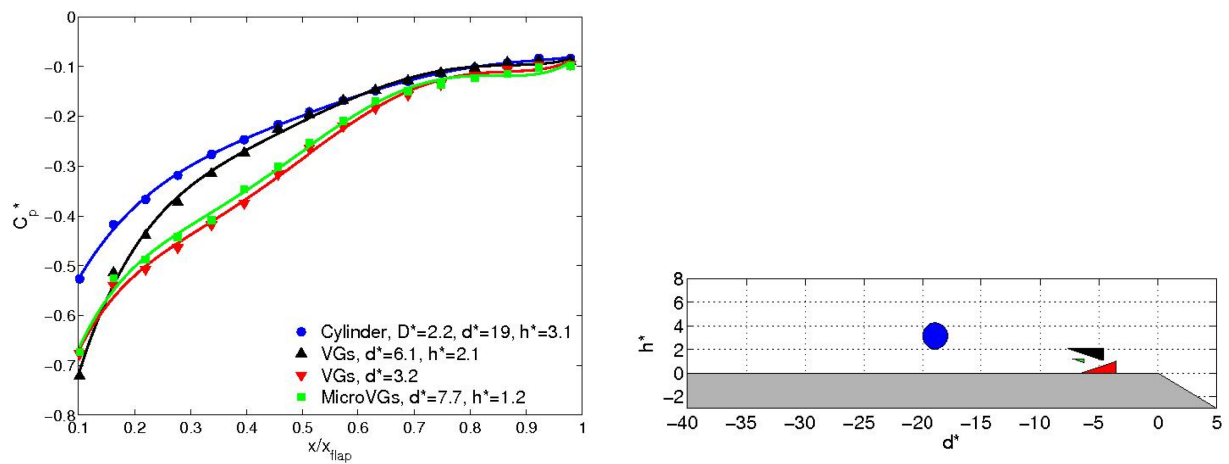


Figure 17. Pressure distributions for the optimum on- and off-surface configurations;  $\phi = 32^\circ$ .

**Table 3. Optimum values for  $d^*$** 

Configuration	$h^* = 1.2^i$	$1.6^{ii}$	$2.1^i$	$3.1^{ii}$	$3.8^i$	$4.9^{ii}$	$6.4^{ii}$
On-surface VGs	On-surface: $d^* = 3.2$						
Off-surface VGs	2.9	-	6.1	-	32	-	-
Off-surface micro VGs	8.5	-	sep	-	sep	-	-
Cylinder $D^* = 0.8$	-	9-12	-	sep	-	sep	sep
Cylinder $D^* = 1.1$	-	sep	-	16-19	-	sep	sep
Cylinder $D^* = 1.5$	-	sep	-	16-19	-	25	sep
Cylinder $D^* = 2.2$	-	sep	-	$6.1^*$ or 19	-	16	19-35

i: VGs; ii: cylinders; -:no tests; sep: separated for all positions; \*: possibly steady effect

flap) with a background contour plot of parameter  $V_{sign}$  which is defined as  $V_{sign} = sign(u)\sqrt{u^2 + w^2}$ . This parameter shows backflow and thus indicates flow separation.

For the  $\phi = 32^\circ$  case where the baseline flow shows separation at the start of the flap, attached flow is obtained when applying either VG's micro VG's and cylinders. Apparently both streamwise and spanwise vortices positioned at the right location with respect to the separation line generated by passive control elements are beneficial for flow separation control.

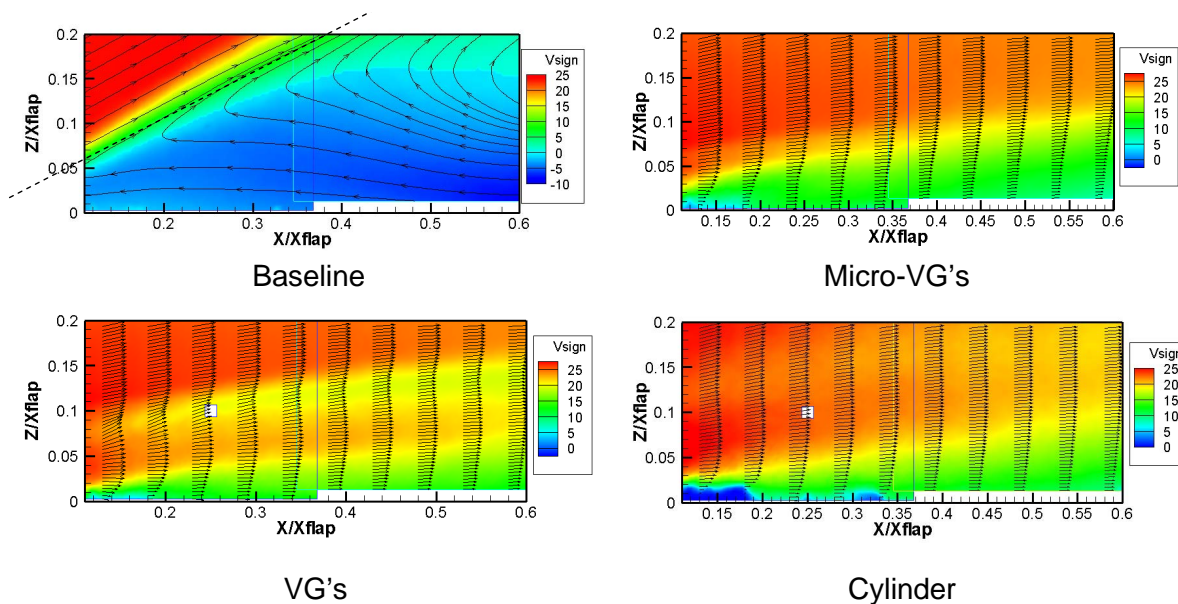


**Figure 18. Comparison of some PIV results for  $\phi = 32^\circ$ . The baseline result shows fully separated flow over the flap while VG's microVG's and cylinders may prevent flow separation by mixing the boundary layer through the generation of vortices.**

## V. Conclusions

The following main conclusions can be drawn, supported by relevant experimental data:

- Pressure and PIV measurements have been performed successfully on a flapped plate airfoil showing large difference between various on-surface and off-surface control elements.
- Off-surface elements have the potential to suppress flow separation efficiently due to the possibility to position them at an optimized location with respect to the separation line. In the case of a wing flap systems the efficiency may improve even further when use can be made of the high energy level gap flow.
- From static pressure measurements and PIV experiments on the flap it was established that for the test case with fully separated flow the off-surface devices were superior to the on-surface vortex generators (with a height of both  $\delta$  and  $\frac{1}{3}\delta$ ). In the flow that was naturally on the verge of separation, off-surface devices were equally effective as on-surface devices. Furthermore, while for the fully separated case the on-surface VGs needed to be placed within  $10\delta$  to the separation point, the off-surface VGs and cylinders maintained attached flow for a distance of over  $30\delta$  to the separation point, provided to height of the devices was chosen correctly.
- For all types of off-surface devices it was found that they performed badly when positioned too close to the separation point, because the vortices did not sufficiently interact with the boundary layer. Typically, the optimum distance for a cylinders was around  $15\delta - 20\delta$  and  $3\delta$  above the wall. For the test case with the boundary layer on the verge of separation, the same distances were found for the off-surface vortex generators, and for the fully separated test case, their optimum position was found to be around  $6\delta$ , and  $2\delta$  above the wall.
- It was found that off-surface vortex generated produce higher intensity vortices than on-surface vortex generators, because the are entirely located in the free stream, outside the boundary layer. The working principle is the same, but because they are generated away from the wall and are initially further away from it, they will suffer less from wall-interactions such as the tendency to be pushed sideways, which would eventually lead to the merging of the vortices.

## References

- <sup>1</sup>M. Gad-el Hak. Flow Control; Passive, Active, and Reactive Flow Management , Cambridge University Press, 2000.
- <sup>2</sup>J. Gilarranz, L. Traub, and O. Rediniotis. Characterization of a Compact, High-Power Synthetic Jet Actuator for Flow Separation Control. 40th AIAA Aerospace Sciences Meeting and Exhibit, 14-17 Januari 2002, AIAA 2002-0127.
- <sup>3</sup>D. Greenblatt and I. Wygnanski. The control of flow separation by periodic excitation. Progress in Aerospace Sciences, 36:487-545, 2000.
- <sup>4</sup>M. van der Steen. Passive Off-Surface Flow Separation Control Methods on a Simplified Flapped Configuration. MSc Thesis, Delft University of Technology, 2009.
- <sup>5</sup>J. Lin. Control of Turbulent Boundary-Layer Separation using Micro-Vortex Generators. 30th AIAA Fluid Dynamics Conference, 28 June - 1 July 1999, AIAA 99-3404.
- <sup>6</sup>P. Ashill, J. Fulker, and K. Hackett. Studies of flows induced by Sub Boundary layer Vortex Generators (SBVGs). 40th AIAA Aerospace Sciences Meeting and Exhibit, 17-21 January 2002. AIAA 2002-0968.
- <sup>7</sup>B. Nishri and I. Wygnanski. Effects of Periodic Excitation on Turbulent Flow Separation from a Flap. AIAA Journal, 36(4):547-556, April 1998.
- <sup>8</sup>L.L.M. Veldhuis and K. Artois. Active Separation Control by Periodic Excitation in an Adverse Pressure Gradient, AIAA-2007-3917, 2007
- <sup>9</sup>M. van der Jagt. Separation Postponement by means of Periodic Surface Excitation, MSc thesis, Delft University of Technology, Faculty of Aerospace Engineering, 2008